

Characterization of adsorbents by energy profile of adsorbed molecules[☆]

Alan L. Myers *, Flor Siperstein

Department of Chemical Engineering, University of Pennsylvania, Philadelphia, PA 19104, USA

Abstract

The energy profile, which is the energy of the adsorbed phase as a function of loading, is essential for characterizing the equilibrium behavior of adsorbents. The energy of the adsorbed phase is measured directly by calorimetry or indirectly by differentiating adsorption isotherms at constant loading. The adsorption isotherm and energy profile are sufficient for the determination of thermodynamic variables such as entropy and provide a basis for predicting the behavior of nonideal, multicomponent mixtures from single-gas isotherms. © 2001 Elsevier Science B.V. All rights reserved.

Keywords: Adsorption; Mixture; Simulation; Energy; Enthalpy

1. Introduction

Adsorption isotherms and pore-size distributions are traditional methods for characterizing adsorbents, but characterization is incomplete without information on energy (or enthalpy). In the same way as a bulk liquid is characterized by its density and enthalpy of vaporization, an adsorbed fluid is characterized by its adsorption isotherm and enthalpy of desorption. However, adsorbates differ from bulk fluids in several sub-

tle but important ways: they possess a surface potential and have zero volume (based upon the Gibbs definition of excess variables). One objective of this paper is to show how the enthalpy profile provides basic information needed to characterize an adsorbent.

Commercial applications of adsorption are based upon adsorption of mixtures. The capacity of adsorbents to purify and separate mixtures depends upon their selectivity or preferential adsorption of one species over another. A second objective of this paper is to show how this selectivity can be predicted, even for highly nonideal systems, from energy profiles. The predictive capacity of single-component adsorption data is important because experimental measurements of the phase equilibria of adsorbed mixtures are difficult and expensive.

[☆] Presented at TRI/Princeton Workshop, 21 June 2000

* Corresponding author. Tel.: +1-215-8987078; fax: +1-215-5732093.

E-mail address: amyers@seas.upenn.edu (A.L. Myers).

2. Adsorption of single gases

The most convenient independent variables for adsorption of single gases are temperature (T) and pressure (P). The key dependent variables are the amount adsorbed (n in mol kg⁻¹) and the integral enthalpy (H in J kg⁻¹) of the adsorbate molecules. All extensive variables (H , n , etc.) are Gibbs excess quantities (Sircar [1]) measured by conventional volumetric, gravimetric, and calorimetric methods.

The nomenclature for enthalpy and isosteric heat is confusing and several different definitions of isosteric heat can be found in the adsorption literature. The heat of adsorption measured experimentally depends upon the imposed conditions, batch; steady state; isothermal; isobaric; etc. Instead of insisting upon a particular path for the definition of isosteric heat, it is advantageous to work with enthalpy, which is a state variable, and therefore, independent of the path. Let the differential enthalpy of desorption ($\Delta\bar{h}$) be the perfect-gas enthalpy minus the differential enthalpy in the adsorbed phase, both at the same temperature. The integral enthalpy of desorption is then:

$$\Delta h = \frac{\int_0^n \Delta\bar{h} \, dn}{n} \quad (1)$$

Eq. (1) shows that the integral enthalpy is not equal to the differential enthalpy unless the latter is constant. Assuming equilibrium adsorption (no hysteresis), it can be shown (Siperstein and Myers [2]) that:

$$\Delta\bar{h} = RT^2 \left(\frac{\partial \ln f}{\partial T} \right)_n \quad (2)$$

The differential enthalpy may be calculated indirectly from adsorption isotherms by Eq. (2) or measured directly by calorimetry (Dunne et al. [3]). For a perfect gas, the fugacity (f) is equal to the pressure (P) and Eq. (2) becomes:

$$\Delta\bar{h} = RT^2 \left(\frac{\partial \ln P}{\partial T} \right)_n \quad (3)$$

The heat of adsorption mentioned most frequently is the isosteric heat:

$$q_{st} = RT^2 \left(\frac{\partial \ln P}{\partial T} \right)_n \quad (4)$$

Comparison of Eqs. (3) and (4) shows that $q_{st} = \Delta\bar{h}$ for the special case of a perfect gas. The differential enthalpy in Eq. (2) is for a real gas and the relation can readily be extended to mixture adsorption. The actual heat of adsorption may be calculated from the differential enthalpy once the path is specified. Here, the emphasis is upon using enthalpy to characterize adsorbents.

The fundamental differential equations for integral adsorption variables are distinguished from bulk-phase thermodynamics by the absence of a PV work term:

$$dH = TdS + \mu \, dn \quad (5)$$

$$dG = -SdT + \mu \, dn \quad (6)$$

However, the integral free energy includes a term for the surface potential (Φ):

$$G = n\mu + \Phi \quad (7)$$

Combination of Eqs. (6) and (7) gives the Gibbs adsorption equation:

$$d\Phi = -SdT - nd\mu \quad (8)$$

The surface potential is evaluated by isothermal integration of Eq. (8):

$$\Phi = - \int_{P=0}^P n \, d\mu \quad (\text{constant } T) \quad (9)$$

For a perfect gas, Eq. (9) becomes:

$$\Phi = -RT \int_0^P \frac{n}{P} dP \quad (\text{constant } T) \quad (10)$$

In summary, the integral enthalpy from Eq. (1) and integral Gibbs free energy from Eq. (7) give the integral entropy:

$$S = \frac{H - G}{T} \quad (11)$$

Entropies calculated from experimental data (Dunne et al. [3,4]) for various molecules adsorbed in silicalite and NaX are plotted on Fig. 1. The entropy (relative to the perfect-gas reference state at the same temperature) becomes infinite at the limit of zero coverage but at saturation $-12 < S/(nR) < -10$. Since the dimensionless

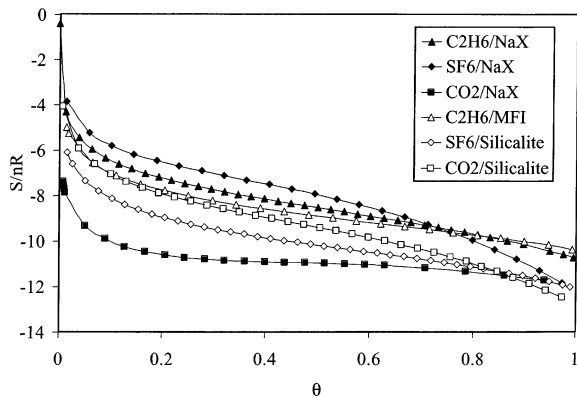


Fig. 1. Integral entropy relative to perfect-gas reference state at 293 K from Eq. (11) for single gases adsorbed on silicalite and NaX. θ is loading expressed as fraction of saturation value. The limit at $\theta = 0$ is ∞ .

entropy of condensation of a vapor at its normal boiling point is -10.5 (Trouton's rule), the entropies of adsorbed gases are close to the entropies of condensed liquids in spite of the fact that the adsorbed gases are near their bulk critical temperatures.

3. Adsorption of multicomponent mixtures

The hypothesis is that multicomponent (binary, ternary, and higher order) adsorption can be predicted with a precision approaching that of experimental measurements from single-gas adsorption isotherms and differential enthalpies (isosteric heats). Two methods are described, (1) empirical correlation of nonideal behavior in the adsorbed phase; and (2) molecular simulation. The success of either method relies heavily upon the accuracy of the experimental data for single-gas adsorption.

Different commercial brands of the same material yield somewhat different values of loading and enthalpy. Even a particular brand of material is sensitive to the degassing protocol used in the experiment. We have avoided the important issue of reproducibility of measurements from different manufacturers and laboratories by using the same sample for the single-gas and mixture experiments.

Adsorption isotherms determined for five gases adsorbed on NaX (Dunne et al. [4]) are shown on Fig. 2. Energy profiles measured by calorimetry for the same gases (Dunne et al. [4]) are shown on Fig. 3. Information plotted on Figs. 2 and 3 can

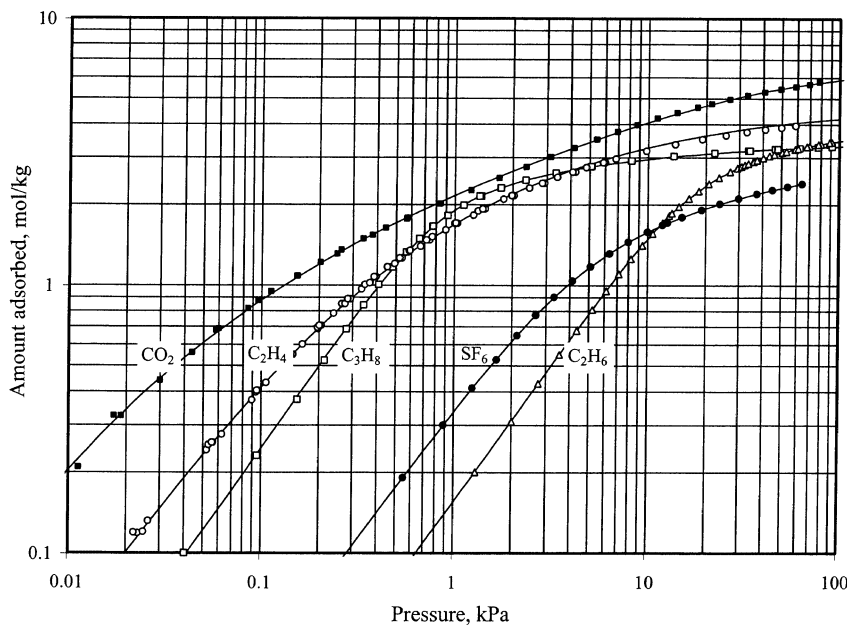


Fig. 2. Experimental adsorption isotherms at 293 K for five gases on NaX.

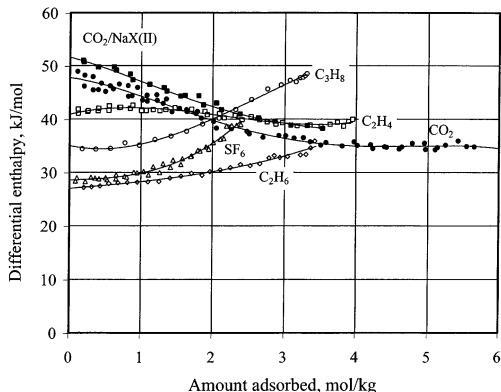


Fig. 3. Experimental differential enthalpies (isosteric heats) at 293 K for five gases on NaX.

be used to predict (nonideal) multicomponent adsorption equilibria on NaX for any combination of these five gases. IAS theory, which is based upon adsorption isotherms alone, requires that the adsorbed mixtures behave ideally. The additional information contained in the energy profiles (Fig. 3) is necessary to predict nonideal multicomponent adsorption.

4. Thermodynamic model for multicomponent equilibria

A thermodynamic model of binary mixture adsorption (Talu et al. [5], Siperstein and Myers [2]) is

$$g^e = (A + BT)(1 - e^{-C\psi})x_1x_2 \quad (12)$$

where A , B , and C are constants specific for a given binary mixture and $\psi = -\Phi/RT$ is a positive quantity with units of loading (mol kg^{-1}). g^e is the excess Gibbs free energy of the adsorbed solution; this excess function is analogous to excess functions in solution thermodynamics of liquid mixtures. Eq. (12) is a master equation from which all properties of the binary mixture can be calculated by thermodynamic relations. Eq. (12) has the built-in limits required of any theory (Talu and Myers [6]), especially thermodynamic consistency and reduction to an ideal solution at the limit of zero loading. Although the excess free

energy has a quadratic (symmetrical) form for the composition dependence at constant surface potential, the composition dependence at constant pressure has the asymmetrical form observed experimentally. The exponential factor for surface potential agrees with experiment and molecular simulation from zero loading up to saturation (Talu et al. [5]).

The composition of the adsorbed phase is calculated from the fugacity equations:

$$Py_i\phi_i = f_i^o\gamma_i x_i \quad (13)$$

where P is pressure, y and x are mole fractions in the gas and adsorbed phases, respectively, ϕ_i is the fugacity coefficient in the gas phase (calculated from an equation of state for the gaseous mixture), f_i^o is the fugacity of the pure component in its standard state defined by ψ , and γ_i is the activity coefficient of component i in the adsorbed phase given by:

$$RT \ln \gamma_i = \left[\frac{\partial(n_i g^e)}{\partial n_i} \right]_{T, \psi, n_j} = (A + BT)(1 - e^{-C\psi})x_j^2 \quad (i \neq j) \quad (14)$$

The linear variation of excess chemical potential with temperature implies an excess enthalpy (heat of mixing), which is independent of temperature:

$$h^e = -T^2 \frac{\partial}{\partial T} \left[\frac{g^e}{T} \right]_{\Phi, x} = A(1 - e^{-C\psi})x_1x_2 \quad (15)$$

an approximation which is consistent with the usual assumption that the differential enthalpies of the pure adsorbates are constant over the temperature range of interest.

The excess reciprocal loading, which vanishes for an ideal solution, is given by:

$$\begin{aligned} \left(\frac{1}{n} \right)^e &= \frac{1}{n_t} - \sum_i \left[\frac{x_i}{n_i^o} \right] = \left[\frac{\partial(g^e/RT)}{\partial \psi} \right]_{T, x} \\ &= \frac{C}{RT} (A + BT) e^{-C\psi} x_1 x_2 \end{aligned} \quad (16)$$

This excess function is required to calculate the total loading (n_t), given the pure-component loadings n_i^o at the same value of ψ as the mixture.

Eqs. (12), (15) and (16) show that the constants A , B , and C are proportional to the excess enthalpy, excess entropy, and excess reciprocal loading, respectively.

In summary, given the pure-component adsorption isotherms and the three constants of Eq. (12) for a binary mixture, setting the pressure (P), temperature (T), and gas composition (y_1) allows the set of fugacity equations to be solved for the unknown values of ψ and x_1 , after which the total loading is calculated from Eq. (16).

5. Correlation of nonideal adsorption of mixtures

The salient properties responsible for nonideal behavior of adsorbed solutions are:

- Difference in differential enthalpy (isosteric heat).
- Difference in integral enthalpy.
- Difference in size of adsorbate molecules.

Fig. 4 shows a dimensionless correlation of the $(A + BT)$ factor in Eq. (12) in terms of these differences. $\Delta\bar{h}^o$ is the differential enthalpy (isosteric heat) at the limit of zero coverage. Component 1 is the one with the larger value of $\Delta\bar{h}^o$ so that $(\Delta\bar{h}_1^o - \Delta\bar{h}_2^o)$ is positive and $(A + BT)$ is negative. $\Delta\bar{h}^s$ is the molar integral enthalpy of desorption evaluated at saturation and V_c is the critical

volume of the adsorbate. Thus the three properties listed above are correlated by $\Delta\bar{h}^o$, $\Delta\bar{h}^s$, and V_c , respectively. The linear correlation in Fig. 4 is:

$$(A + BT) = - (0.188) \left(\frac{\Delta\bar{h}_2^s}{\Delta\bar{h}_1^s} \right) \left(\frac{V_{c2}}{V_{c1}} \right) (\Delta\bar{h}_2^o - \Delta\bar{h}_1^o) \quad (17)$$

For purposes of correlation, the mixture saturation capacity (m_{12}) at the equimolar composition ($x_1 = 0.5$) is:

$$\frac{1}{m_{12}} = \frac{0.5}{m_1} + \frac{0.5}{m_2} \quad (18)$$

Fig. 5 shows that the constant C is correlated with m_{12} . The solid line on Fig. 5 is represented by the equation:

$$C = \frac{31.8}{m_{12}^{3.96}} \quad (19)$$

for C in kg mol^{-1} and m_{12} in mol kg^{-1} .

The mixtures listed in Table 1 (Dunne et al. [7], Siperstein and Myers [2]) cover the full range of behavior from ideal to highly nonideal. The two extremes are the $\text{C}_2\text{H}_6/\text{CH}_4$ mixture on silicalite,

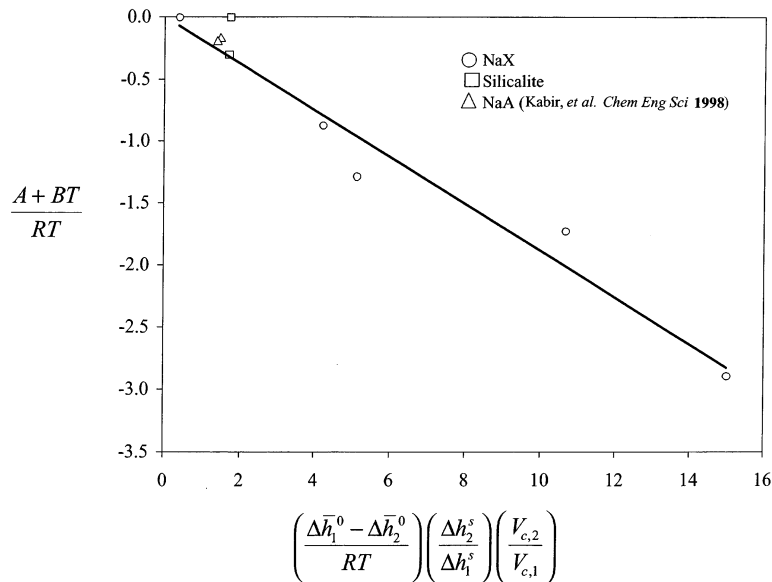


Fig. 4. Correlation of $(A + BT)$ in Eq. (12) with pure-component properties. $\Delta\bar{h}^o$ is the differential enthalpy at the limit of zero loading; $\Delta\bar{h}^s$ is the molar integral enthalpy from Eq. (1) evaluated at saturation; V_c is the critical volume of the gas.

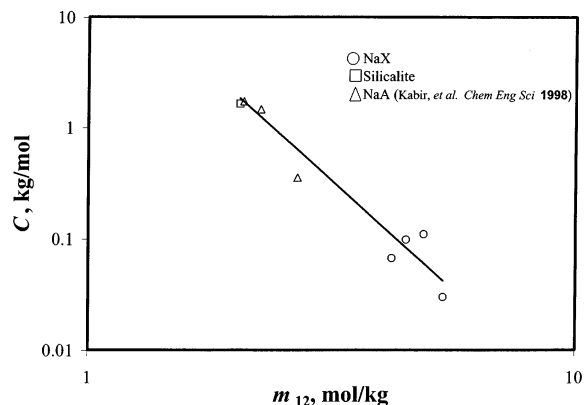


Fig. 5. Correlation of C in Eq. (12) with saturation capacity m_{12} from Eq. (18).

which is ideal, and the $\text{CO}_2/\text{C}_3\text{H}_8$ mixture on NaX, which has activity coefficients at infinite dilution below 0.1 and a heat of mixing of -2900 J mol^{-1} at the equimolar composition. The correlations represented by Eqs. (17) and (19) are compared with experiment on Fig. 6; the agreement is within the estimated experimental error.

In addition to the binary mixtures, experiments were performed for ternary adsorption of $\text{CO}_2/\text{C}_2\text{H}_4/\text{C}_2\text{H}_6$ on NaX (Siperstein and Myers [2]). Our assumption of a quadratic dependence for the excess functions of binary mixtures implies the dominance of pairwise interactions, so Eq. (12) can be extended to multicomponent (ternary and higher order) systems by adding terms for the constituent binaries. Specifically, for a ternary system:

$$g^e = (A_{12} + B_{12}T)(1 - e^{-C_{12}\psi})x_1x_2 + (A_{13} + B_{13}T)(1 - e^{-C_{13}\psi})x_1x_3 + (A_{23} + B_{23}T)(1 - e^{-C_{23}\psi})x_2x_3 \quad (20)$$

Fig. 7 shows a comparison of experimental ternary selectivities with values calculated from Eq. (20) using binary parameters from Eqs. (17)

and (19). The good agreement confirms the validity of the correlation and the assumption of pairwise interactions inherent in Eq. (20). In summary, it has been shown that binary and ternary mixture equilibria can be predicted from single-component isotherms and energy profiles (isosteric heat versus loading).

6. Prediction of nonideal adsorption by molecular simulation

The correlation of nonideal adsorption by Eqs. (17) and (19) is based upon accurate experimental data for single-component adsorption isotherms and enthalpies. In principle, it should be possible to extract realistic intermolecular potentials from the single-component data and then predict the mixture equilibria by molecular simulation.

The simulation approach was tested for binary mixtures of SF_6 and CH_4 on NaX. The molecular model was a Lennard–Jones 12-6 potential for both the gas–solid and gas–gas interactions. Both SF_6 and CH_4 were represented as spherical molecules using the parameters in Table 2. We adopted the customary approximation of ignoring the less accessible silicon atoms and calculating

Table 1
Binary gas mixtures studied

Type of system	Adsorbent	Adsorbate 1	Adsorbate 2
Homogeneous, size difference	Silicalite	SF_6	CH_4
Homogeneous, ideal	Silicalite	C_2H_6	CH_4
Heterogeneous, polar–nonpolar	NaX	CO_2	C_2H_6
Heterogeneous, polar–nonpolar	NaX	CO_2	C_3H_8
Heterogeneous, polar–nonpolar	NaX	C_2H_4	C_2H_6
Heterogeneous, nonpolar–nonpolar	NaX	SF_6	C_2H_6
Heterogeneous, polar–polar	NaX	CO_2	C_2H_4

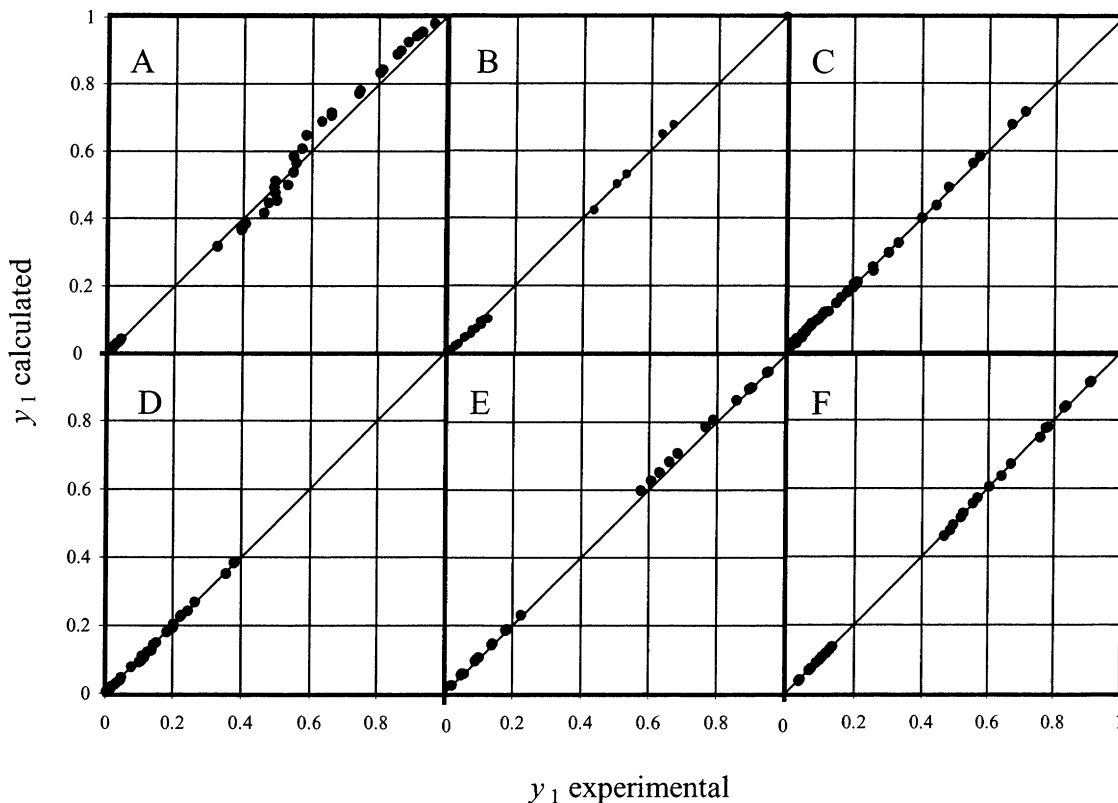


Fig. 6. Comparison of correlation with experiment for vapor composition y_1 . Independent variables are total loading (n_1) and composition of adsorbed phase (x_1). (A) $\text{CO}_2\text{-C}_3\text{H}_8$ on NaX; (B) $\text{CO}_2\text{-C}_2\text{H}_6$ on NaX; (C) $\text{C}_2\text{H}_4\text{-C}_2\text{H}_6$ on NaX; (D) $\text{SF}_6\text{-CH}_4$ on silicalite; (E) $\text{SF}_6\text{-C}_2\text{H}_6$ on NaX; (F) $\text{CO}_2\text{-C}_2\text{H}_4$ on NaX.

dispersion energy as if only oxygen atoms were present at the locations given by crystallographic data (Olson et al. [8]). The simulation box was 12 units cells of silicalite, which is approximately 40 Å on a side (Talu and Myers [9]). The fit of the simulation to experiment is shown in Figs. 8 and 9. The fitted isotherms are in excellent agreement with experiment but there is an average error of about 2 kJ mol^{-1} in the differential enthalpies for SF_6 .

It is emphasized that the potential parameters quoted in Table 2 were optimized for agreement with experiment. Forcing the gas–gas and gas–solid potentials to fit the single-component experimental data is a necessary preliminary step for the prediction of mixture properties.

Mixture simulations using potential parameters

from Table 2 are compared with experiment in Fig. 10. The customary Lorentz–Berthelot mixing rules were used to calculate the $\text{CH}_4\text{-SF}_6$ interactions; no mixture data were used to predict the nonideal behavior of the system shown in Fig. 10. The excess free energy shows moderate negative deviations from ideality and the agreement of simulation with experiment is excellent.

The successful prediction of nonideal behavior for adsorbed mixtures of $\text{SF}_6\text{-CH}_4$ from ‘ideal’ Lorentz–Berthelot mixing rules may seem surprising at first sight. However, the source of the nonidealities is not the gas–gas interactions but the gas–solid interactions. The unequal competition of SF_6 and CH_4 for high-energy adsorption sites causes segregation in the adsorbed phase, so that the local composition varies with position

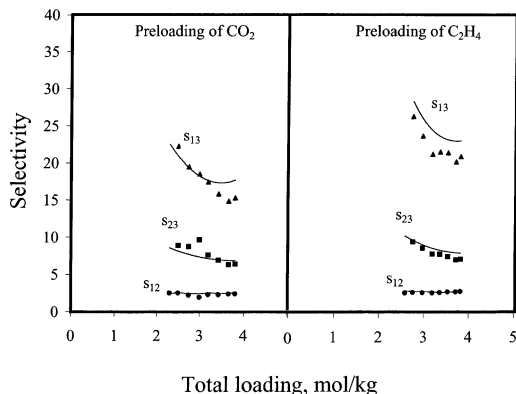


Fig. 7. Comparison of correlation (solid lines) with experiment (points) for the ternary system CO_2 (1) – C_2H_4 (2) – C_2H_6 (3) on NaX. Selectivity $s_{ij} = (x_i y_j)/(x_j y_i)$. Ternary free energy calculated from Eq. (20).

inside the supercage and its windows. This large difference in local composition is the reason for negative deviations from Raoult's law (Myers [10]).

7. Conclusions

The energy profile for adsorption of single gases is essential for characterizing adsorbents and for predicting nonideal mixture equilibria.

The three-constant thermodynamic model for the excess free energy of mixing in the adsorbed phase, Eq. (12), provides a quantitative description of mixture adsorption equilibria.

Multicomponent adsorption equilibria can be predicted from the correlations of Eqs. (17) and (19). Alternatively, multicomponent adsorption equilibria can be predicted by molecular simula-

Table 2
Potential parameters used for molecular simulations in Figs. 8 and 9

Pair	ϵ/k (K)	σ (Å)
$\text{CH}_4\text{--CH}_4$	151.2	3.739
$\text{SF}_6\text{--SF}_6$	252.4	4.900
$\text{CH}_4\text{--SF}_6$	195.4	4.320
$\text{CH}_4\text{--O}$	104.5	3.502
$\text{SF}_6\text{--O}$	118.7	4.085

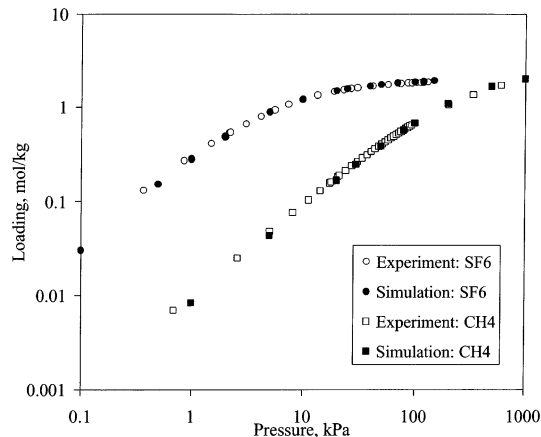


Fig. 8. Comparison of simulation with experiment for single-gas adsorption isotherms of SF_6 (circles) and CH_4 (squares) on NaX at 25°C. Open symbols: experiment; closed symbols: simulation.

tion. Both approaches, correlation and simulation, require accurate adsorption isotherms and differential enthalpies (isosteric heats) for the single components. Use of the same adsorbent sample for the single gases and the mixture avoids the problem of reproducibility of results for different brands and batches of adsorbent.

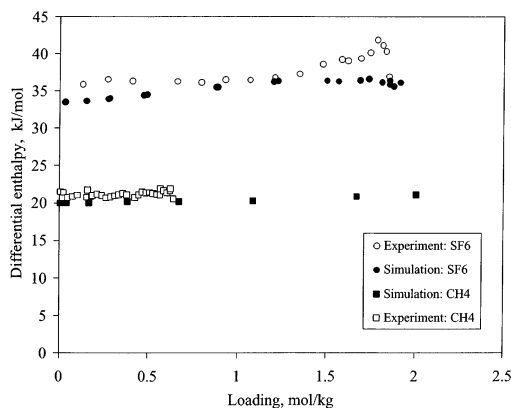


Fig. 9. Comparison of simulation with experiments for differential enthalpies of SF_6 and CH_4 on NaX at 25°C. Legend same as Fig. 8.

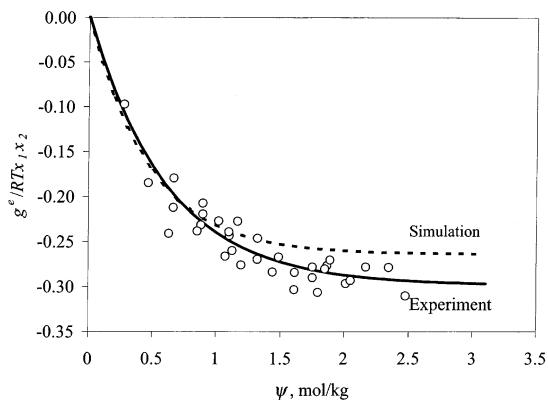


Fig. 10. Comparison of simulation with experiment for excess free energy of mixtures of SF_6 and CH_4 on NaX at 25°C as a function of surface potential ψ .

Acknowledgements

This research was supported by Air Products

and Chemicals, Inc. and by National Science Foundation Grant NSF CTS 96–10030.

References

- [1] S. Sircar, *J. Chem. Soc. Faraday Trans.* 81 (1985) 1527.
- [2] F.R. Siperstein, A.L. Myers, 'Mixed-gas adsorption', *AIChE J.*, in press (2001).
- [3] J.A. Dunne, R. Mariwala, M. Rao, S. Sircar, R.J. Gorte, A.L. Myers, *Langmuir* 12 (1996) 5888.
- [4] J.A. Dunne, M. Rao, S. Sircar, R.J. Gorte, A.L. Myers, *Langmuir* 12 (1996) 5896.
- [5] O. Talu, J. Li, A.L. Myers, *Adsorption* 1 (1995) 103.
- [6] O. Talu, A.L. Myers, *AIChE J.* 34 (1988) 1887.
- [7] J.A. Dunne, M. Rao, S. Sircar, R.J. Gorte, A.L. Myers, *Langmuir* 13 (1997) 4333.
- [8] D.H. Olson, G.T. Kokotailo, S.L. Lawton, W.M. Meier, *J. Phys. Chem.* 85 (1981) 2238.
- [9] O. Talu, A.L. Myers, 'Molecular Simulation of Adsorption: Gibbs Dividing Surface and Comparison with Experiment', *AIChE J.*, in press (2001).
- [10] A.L. Myers, *AIChE J.* 29 (1983) 691.